0026-895X/11/8006-1066–1075$25.00
MOLECULAR PHARMACOLOGY
Vol. 80, No. 6
71761/3730050
*Mol Pharmacol* 80:1066–1075, 2011
*Printed in U.S.A.*




# $Ca^{2+}$/Calmodulin-Dependent Kinase (CaMK) Signaling via CaMKI and AMP-Activated Protein Kinase Contributes to the Regulation of WIPI-1 at the Onset of Autophagy[S]

Simon G. Pfisterer, Mario Mauthe, Patrice Codogno, and Tassula Proikas-Cezanne

*Autophagy Laboratory, Interfaculty Institute for Cell Biology, Eberhard Karls University Tuebingen, Tuebingen, Germany (S.G.P., M.M., T.P.-C.); and Institut National de la Santé et de la Recherche Médicale U984, Faculté de Pharmacie, University Paris-Sud 11, Châtenay-Malabry, France (P.C.)*

Received February 14, 2011; accepted September 6, 2011

## ABSTRACT

Autophagy is initiated by multimembrane vesicle (autophagosome) formation upon mammalian target of rapamycin inhibition and phosphatidylinositol 3-phosphate [PtdIns(3)P] generation. Upstream of microtubule-associated protein 1 light chain 3 (LC3), WD-repeat proteins interacting with phosphoinositides (WIPI proteins) specifically bind PtdIns(3)P at forming autophagosomal membranes and become membrane-bound proteins of generated autophagosomes. Here, we applied automated high-throughput WIPI-1 puncta analysis, paralleled with LC3 lipidation assays, to investigate $Ca^{2+}$-mediated autophagy modulation. We imposed cellular stress by starvation or administration of etoposide (0.5–50 $\mu$M), sorafenib (1–40 $\mu$M), staurosporine (20–500 nM), or thapsigargin (20–500 nM) (1, 2, or 3 h) and measured the formation of WIPI-1 positive autophagosomal membranes. Automated analysis of up to 5000 individual cells/treatment demonstrated that $Ca^{2+}$ chelation by BAPTA-AM (10 and 30 $\mu$M) counteracted starvation or pharmacological compound-induced WIPI-1 puncta formation and LC3 lipidation. Application of selective $Ca^{2+}$/calmodulin-dependent kinase kinase (CaMKK) $\alpha/\beta$ and calmodulin-dependent kinase (CaMK) I/II/IV inhibitors 7-oxo-7*H*-benzimidazo[2,1-*a*]benz[*de*]isoquinoline-3-carboxylic acid acetate (STO-609; 10–30 $\mu$g/ml) and 2-(*N*-[2-hydroxyethyl])-*N*-(4-methoxybenzenesulfonyl)amino-*N*-(4-chlorocinnamyl)-*N*-methylamine (KN-93; 1–10 $\mu$M), respectively, significantly reduced starvation-induced autophagosomal membrane formation, suggesting that $Ca^{2+}$ mobilization upon autophagy induction involves CaMKI/IV. By small interefering RNA (siRNA)-mediated down-regulation of CaMKI or CaMKIV, we demonstrate that CaMKI contributes to stimulation of WIPI-1. In line, WIPI-1 positive autophagosomal membranes were formed in AMP-activated protein kinase (AMPK) $\alpha_1/\alpha_2$-deficient mouse embryonic fibroblasts upon nutrient starvation, whereas basal autophagy was prominently reduced. However, transient down-regulation of AMPK by siRNA resulted in an increased basal level of both WIPI-1 puncta and LC3 lipidation, and nutrient-starvation induced autophagy was sensitive to STO-609/KN-93. Our data provide evidence that pharmacological compound-modulated and starvation-induced autophagy involves $Ca^{2+}$-dependent signaling, including CaMKI independent of AMPK$\alpha_1/\alpha_2$. Our data also suggest that AMPK$\alpha_1/\alpha_2$ might differentially contribute to the regulation of WIPI-1 at the onset of autophagy.

## Introduction

Autophagy is a lysosomal bulk degradation system for cytoplasmic constituents, including long-lived proteins and organelles. This process of self-digestion is constitutively active (basal autophagy) and promotes the recycling of the cytoplasm, thereby supplying macromolecules and energy for metabolic reactions (e.g., Klionsky et al., 2007). Upon cellular

This study was supported by the Deutsche Forschungsgemeinschaft [Grants SFB773, A03] and the Bundesministerium für Bildung und Forschung [Grant FKZ 031 3816B].

Article, publication date, and citation information can be found at http://molpharm.aspetjournals.org.

doi:10.1124/mol.111.071761.

[S] The online version of this article (available at http://molpharm.aspetjournals.org) contains supplemental material.

**ABBREVIATIONS:** PtdIns3KC3, phospatidylinositol-3 kinase class III; TORC1, mTOR complex 1; LC3, microtubule-associated protein 1 light chain 3; PtdIns(3)P, phosphatidylinositol 3-phosphate; WIPI, WD-repeat protein interacting with phosphoinositides; mTOR, mammalian target of rapamycin; CaMK, calmodulin-dependent kinase; CaMKK, calmodulin-dependent kinase kinase; AMPK, AMP-activated protein kinase; STO-609, 7-oxo-7*H*-benzimidazo[2,1-*a*]benz[*de*]isoquinoline-3-carboxylic acid acetate; KN-93, 2-(*N*-[2-hydroxyethyl])-*N*-(4-methoxybenzenesulfonyl)amino-*N*-(4-chlorocinnamyl)-*N*-methylamine; Baf, bafilomycin; DAPI, 4,6-diamidino-2-phenylindole; BAPTA-AM, 1,2-bis(2-aminophenoxy)ethane-*N*,*N*,*N*′,*N*′-tetraacetic acid acetoxymethyl ester; DMEM, Dulbecco's modified Eagle's medium; FCS, fetal calf serum; GFP, green fluorescent protein; MEF, mouse embryonic fibroblast; SF, sorafenib; SP, staurosporine; TG, thapsigargin; EP, etoposide; NF, nutrient-free medium lacking amino acids and serum; CM, control medium; WM, wortmannin; WT, wild-type; LY294002, 2-(4-morpholinyl)-8-phenyl-4*H*-1-benzopyran-4-one.

stress such as nutrient starvation, autophagy is induced above basal level and critically secures cellular survival. This cytoprotective function is compromised in a variety of age-related human diseases, hence modulating autophagy as a new therapeutic strategy has attracted attention over the last few years (Kondo et al., 2005; Mizushima et al., 2008; Fleming et al., 2011). For this aim, vital molecular details need to be addressed, such as the molecular understanding of contributing signaling pathways that regulate autophagy (Codogno et al., 1997; Chen and Klionsky, 2011).

During the process of autophagy, multimembrane vesicles, autophagosomes, are formed from initial membrane templates (phagophore) that begin to sequester the cytoplasmic cargo; formed autophagosomes fuse with lysosomes to autolysosomes where cargo degradation takes place (e.g., Klionsky and Emr, 2000). Autophagosome formation is regulated by the activity of TORC1, PtdIns3KC3 complex I, and PtdIns(3)P effectors; two ubiquitin-like conjugation systems (Atg12-Atg5 and LC3); and the Atg9 pathway, which contributes to the delivery of membrane sources (e.g., Noda et al., 2010). Ubiquitin-like conjugation systems contribute to the elongation of early autophagosomal membranes, where LC3 is conjugated to phosphatidylethanolamine (LC3 lipidation), promoting membrane tethering and hemifusion (Ohsumi 2001; Nakatogawa et al., 2007). Monitoring LC3 lipidation is used to score for autophagosome formation, and the addition of lysosomal inhibitors provides further information regarding the autophagic flux (Rubinsztein et al., 2009). The initiation of autophagosome formation is critically governed by TORC1, which inhibits autophagy; consequently, TORC1 inhibitors (e.g., rapamycin) induce autophagy (Blommaart et al., 1995). Crucial for the formation of autophagosomes is the activation of the PtdIns3KC3 complex I, including Beclin 1, Vps15, and Atg14L, which generates PtdIns(3)P, an essential phospholipid for autophagosomal membrane formation (Petiot et al., 2000; Matsunaga et al., 2009). Consequently, compounds that inhibit PtdIns(3)P generation (e.g., wortmannin) abolish autophagosome formation (Blommaart et al., 1997).

We previously identified the human WIPI family, including WIPI-1 (Atg18 in yeast), which functions as a PtdIns(3)P effector at early autophagosomal membranes (Proikas-Cezanne et al., 2004, 2007). The specific autophagosomal membrane localization of PtdIns(3)P-bound WIPI-1 is inhibited by wortmannin (Proikas-Cezanne et al., 2004) and PtdIns3KC3 down-regulation (Itakura and Mizushima, 2010), suggesting that WIPI-1 binds PtdIns(3)P generated by the PtdIns3KC3 complex I (Nobukuni et al., 2007). Rapamycin-mediated TORC1 inhibition also stimulates WIPI-1 to localize at early autophagosomal membranes, suggesting that WIPI-1 also acts downstream of mTOR activity (Proikas-Cezanne et al., 2007). To use WIPI-1 for monitoring autophagy in human cells, we employ quantitative, fluorescence-based WIPI-1 puncta-formation analyses in which basal autophagy is reflected by the number of cells that display WIPI-1 at autophagosomal membranes (WIPI-1 puncta), and induced or inhibited autophagy is reflected by the elevated or decreased number of cells displaying WIPI-1 puncta.

In this study, we used WIPI-1 puncta-formation and quantitative LC3 lipidation analyses to provide molecular details on cytosolic $Ca^{2+}$ increase-mediated modulation of autophagy. Several studies have analyzed the role of $Ca^{2+}$ with regard to the regulation of autophagy; however, whether $Ca^{2+}$ contributes to the activation or inhibition of autophagy is still under investigation (Demarchi et al., 2006; Brady et al., 2007; Høyer-Hansen et al., 2007; Williams et al., 2008; Grotemeier et al., 2010; Khan and Joseph, 2010; Fleming et al., 2011). Cytoplasmic $Ca^{2+}$ is bound by calmodulin, which associates to and activates calmodulin-dependent kinase kinase $\alpha/\beta$ (CaMKK$\alpha/\beta$), leading to AMPK stimulation and subsequent TORC1 inhibition (Hardie, 2008; Means, 2008). This notion implies that autophagy might be activated by $Ca^{2+}$/calmodulin–CaMKK$\alpha/\beta$–AMPK–TORC1 signaling. In fact, evidence that calcium signaling contributes to the induction of autophagy was provided by using compounds that elevate cytosolic $Ca^{2+}$, such as thapsigargin (Høyer-Hansen et al., 2007). We previously found that $Ca^{2+}$-mediated induction of autophagy can also bypass AMPK (Grotemeier et al., 2010), suggesting that additional routes downstream of $Ca^{2+}$/calmodulin could activate autophagy. Because it is known that the $Ca^{2+}$/calmodulin signal also activates CaMKI/II/IV apart from AMPK (Means, 2008), we asked in this study whether or not this route might contribute to the regulation of autophagy. Herein, we provide evidence that nutrient starvation and pharmacological compound-modulated autophagy mobilizes cellular $Ca^{2+}$, in part via CaMKI independent of AMPK, to regulate the PtdIns(3)P effector WIPI-1, and LC3.

## Materials and Methods

**Reagents.** Earle's balanced salt solution, etoposide ($C_{29}H_{32}O_{13}$, CAS 33419-42-0), 2-(*N*-[2-hydroxyethyl])-*N*-(4-methoxybenzenesulfonyl)amino-*N*-(4-chlorocinnamyl)-*N*-methylamine (KN-93; $C_{26}H_{29}ClN_2O_4S{\cdot}H_3PO_4$, CAS 139298-40-1), staurosporine ($C_{28}H_{26}N_4O_3$, CAS 62996-74-1), 7-oxo-7*H*-benzimidazo[2,1-*a*]benz[*de*]isoquinoline-3-carboxylic acid acetate (STO-609; $C_{19}H_{10}N_2O_3{\cdot}C_2H_4O_2$, CAS 52029-86-4), thapsigargin ($C_{34}H_{50}O_{12}$, CAS 67526-95-8), and wortmannin ($C_{23}H_{24}O_8$, CAS 19545-26-7) were obtained from Sigma-Aldrich (St. Louis, MO); sorafenib ($C_{21}H_{16}ClF_3N_4O_3{\cdot}C_7H_8O_3S$, CAS 475207-59-1) from Selleck Chemicals (Houston, TX); Baf $A_1$ (bafilomycin $A_1$; $C_{35}H_{58}O_9$, CAS 88899-55-2) and DAPI ($C_{16}H_{15}N_5{\cdot}2HCl$, CAS 28718-90-3) from AppliChem (Darmstadt, Germany); and BAPTA-AM ($C_{34}H_{40}N_2O_{18}$; CAS 126150-97-8) from Invitrogen (Carlsbad, CA). Anti-AMPK-$\alpha$ and anti-CaMKIV antibodies were purchased from Cell Signaling Technology (Danvers, MA); anti-CaMKI, anti-LC3, and anti-$\alpha$-tubulin antibodies from Abcam Inc. (Cambridge, MA), nanoTools (Teningen, Germany), and Sigma-Aldrich, respectively. Anti-WIPI-1 antiserum was described previously (Proikas-Cezanne et al., 2004). Anti-rabbit IgG-Alexa Fluor 546 and TO-PRO-3 was obtained from Invitrogen.

**DNA.** GFP-WIPI-1 was described previously (Proikas-Cezanne et al., 2007). GFP-ULK2 was generated by cloning human ULK2 cDNA (*imaGenes* clone IRATp970B0931D) into pEGFP.C1 (XhoI). Construct integrity was confirmed by PCR, automated DNA sequencing, and protein expression analysis.

**siRNA.** Control siRNA and human AMPK$\alpha_1/\alpha_2$ siRNA were purchased from Santa Cruz Biotechnology (Santa Cruz, CA). Control, human CaMKI or CaMKIV endoribonuclease-prepared siRNAs were obtained from Sigma-Aldrich.

**Cell Culture.** Human U2OS osteosarcoma cell line (American Type Culture Collection, Manassas, VA) and human G361 malignant melanoma cell line (American Type Culture Collection) were cultured in Dulbecco's modified Eagle's medium (DMEM), 10% FCS, 100 U/ml penicillin/100 $\mu$g/ml streptomycin, and 5 $\mu$g/ml Plasmocin (InvivoGen, San Diego, CA) at 37°C, 5% $CO_2$. Stable U2OS clones expressing GFP-WIPI-1 were cultured in DMEM, 10% FCS, 100 U/ml penicillin/100 $\mu$g/ml streptomycin, and 5 $\mu$g/ml Plasmocin (InvivoGen) supplemented with 0.6 mg/ml G418 (Invitrogen) (Grotemeier et al., 2010). AMPK$\alpha_1/\alpha_2$-deficient and wild-type mouse embryonic fibroblasts (MEF) were cultured as described previously

(Laderoute et al., 2006) in DMEM/10% FCS supplemented with 25 mM HEPES, pH 7.2 to 7.5, 50 $\mu$M $\beta$-mercaptoethanol, and 100 $\mu$M nonessential amino acids (all from Invitrogen).

**Transfections.** Transient transfections were conducted by using Promofectine (PromoCell, Heidelberg, Germany) for DNA plasmids, or by using RNAiMax (Invitrogen) for siRNAs according to the manufacturer's protocols. Three hours after transfection, the transfection medium of AMPK$\alpha_1/\alpha_2$-deficient and wild-type MEFs was replaced by normal culture medium (see *Cell Culture*) with either 4.5, 1.0, or 0.1 g/L glucose.

**Treatments.** Cells were treated for 1 to 3 h with thapsigargin (0.02–0.5 $\mu$M), staurosporine (0.02–0.5 $\mu$M), sorafenib tosylate (1–40 $\mu$M), etoposide (0.5–50 $\mu$M), or wortmannin (233 nM) or by amino acid and serum deprivation (Earle's balanced salt solution, nutrient-free medium). To inhibit the autophagic flux, cell culture medium was supplemented with bafilomycin $A_1$ (200 nM). To chelate, cytoplasmic $Ca^{2+}$ cells were pretreated with BAPTA-AM (10–30 $\mu$M). For CaMKK and CaMK inhibition with STO-609 and KN-93, cells were pretreated for 30 min and autophagy assays were performed for 1 h.

**Quantitative Confocal Microscopy.** Quantitative confocal microscopy of GFP-WIPI-1 puncta-positive cells using a laser-scanning microscope (LSM 510; Carl Zeiss GmbH, Jena, Germany) and a 63×, 1.4 numerical aperture, differential interference contrast, Plan-Apochromat, oil-immersion objective was performed as described previously (Proikas-Cezanne et al., 2007).

**Automated High-Throughput Image Acquisition and Analyses.** Stable U2OS GFP-WIPI-1 cells were cultured in 96-well plates. Cells were treated as indicated, fixed in 3.7% paraformaldehyde, and stained with DAPI (5 $\mu$g/ml in phosphate-buffered saline). An automated imaging platform equipped with a Nikon Plan Fluor ELWD 40 × 0.6 objective was used for automated image acquisition (In Cell Analyzer 1000; GE Healthcare, Chalfont St. Giles, Buckinghamshire, UK) and analyses (In Cell Analyzer Workstation 3.4). Twenty images per well (approximately 20 cells per image) were routinely acquired from each experimental treatment, and the dual area object assay used to classify cells as WIPI-1 puncta-positive or -negative (see Fig. 1). Applying a decision tree to automatically analyze the acquired images (Grotemeier et al., 2010), cells were detected by using DAPI (cell nuclei) and corresponding GFP images. Using the parameters inclusion size and intensity versus cell intensity, cells were further classified to measure the resulting GFP-WIPI-1 puncta-positive or puncta-negative cells. High-intensity GFP inclusions (terminology from Workstation 3.4), counted per puncta-positive cell, provided the measure of the average of GFP-WIPI-1 puncta per puncta-positive cell.

**Quantitative LC3 Immunoblotting.** Cells were washed twice with phosphate-buffered saline and lysed with Tris-buffered saline/1% Triton X-100. Cell lysates were centrifuged at 15,000*g* for 10 min at 4°C to remove nuclei and cell debris. Supernatants were mixed with 4× Laemmli loading buffer (200 mM Tris, pH 6.8, 5 mM EDTA, pH 8.0, 50% glycerol, 8% SDS, 200 mM dithiothreitol, 10% $\beta$-mercaptoethanol, and 0.1% bromphenol blue). Alternatively, cells were lysed by using hot Laemmli buffer, and the chromatin was disintegrated by using a 23-gauge needle. Protein extracts were subjected to SDS-polyacrylamide gel electrophoresis and Western blot analysis using anti-LC3 and anti-$\alpha$-tubulin antibodies. Quantifications of Western blot results were conducted using ImageQuant 5.1 (GE Healthcare), and LC3-II signal intensities were normalized over tubulin.

**Statistical Analyses.** *p* Values were calculated by using two-tailed heteroscedastic *t*-testing.

## Results

**Automated GFP-WIPI-1 Puncta-Formation Analysis Monitors PtdIns(3)P-Dependent Autophagy Modulated by Pharmacological Compound Administration.** WIPI-1 puncta-formation analysis is used to assess PtdIns(3)P-

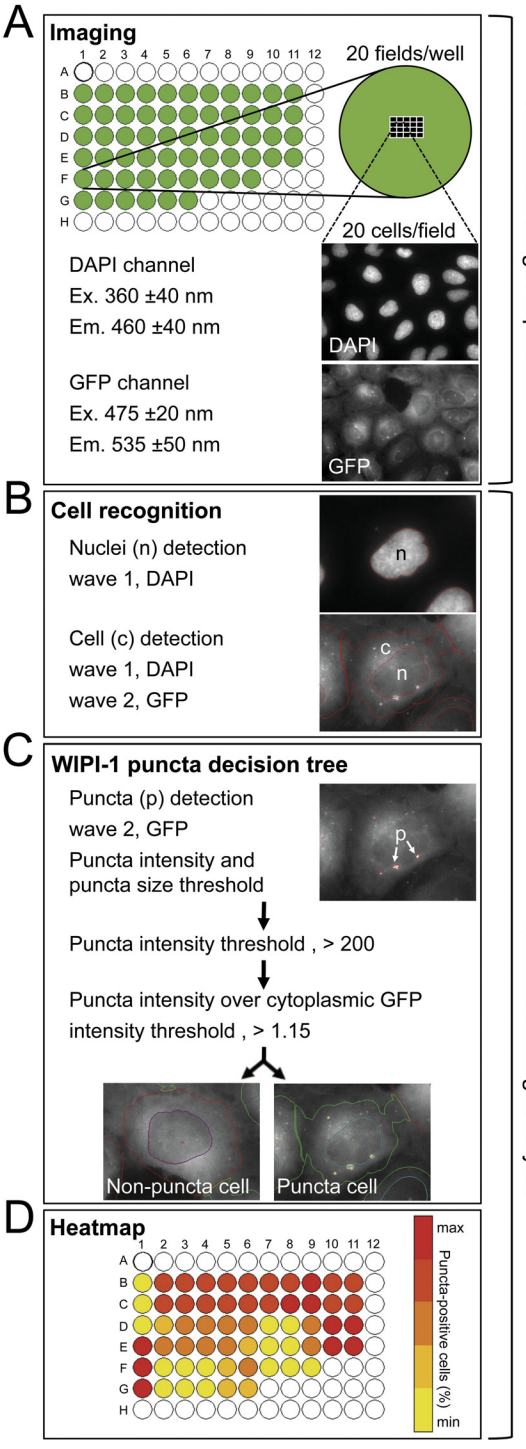


**Fig. 1.** Automated high-throughput WIPI-1 puncta image acquisition and analysis using stable GFP-WIPI-1 U2OS osteosarcoma cells. Images of treated cells in 96-well plates were automatically acquired using DAPI and GFP fluorescence (A). Twenty image fields were acquired per well, each field displaying ~20 cells (A). Automated image analysis is based on cell (B) and GFP-WIPI-1 puncta (C) recognition. From three independent experiments, up to 5000 individual cells per treatment are routinely analyzed (Figs. 2–6). During automated image analysis, a dynamic heat map monitors the number of GFP-WIPI-1 puncta-positive cells (D). Subsequently, data are extracted, statistically analyzed (Figs. 2–6), and expressed as the number of WIPI-1 puncta per cell area and/or the number of puncta-positive cells. *p* Values were calculated on the basis of mean values from independent wells (Figs. 2–4) or image fields (Figs. 5 and 6).

dependent mammalian autophagy established for visualizing endogenous WIPI-1 or overexpressed variants of tagged WIPI-1 proteins followed by quantitative fluorescence microscopy (Proikas-Cezanne et al., 2007). In this study, we employed our recently established procedure for automated GFP-WIPI-1 puncta image acquisition and analysis (Grotemeier et al., 2010). In brief, stable GFP-WIPI-1 U2OS cells were assayed in 96-well plates and fixed, and cell nuclei stained with DAPI. GFP and DAPI images were automatically acquired in each field (20 cells/field; 20 fields/well) (Fig. 1A). Automated quantitative analyses included the recognition of 1) individual cells (Fig. 1B) by using both DAPI and GFP images (~400 cells/well), and 2) GFP-WIPI-1 puncta by applying a decision tree based on puncta intensity and size thresholds (Fig. 1C). During image analyses, a dynamic heat map presents the range of GFP-WIPI-1 puncta-positive cells detected per well (Fig. 1D). Here, we analyzed up to 5100 individual cells per treatment from two to six independent experiments (Figs. 2, 3A, 3B, 3C, 4, 5B, 5C, 6B, 6C). Using this system, we assessed the effects of the anticancer drugs sorafenib (SF) and etoposide (EP), the pan-kinase inhibitor staurosporine (SP), and the sarco(endo)plasmic reticulum $Ca^{2+}$ ATPase inhibitor thapsigargin (TG) on WIPI-1 puncta formation (Fig. 2). Because it has been demonstrated that serum influences compound effects on autophagy (Yang et al., 2010), we conducted the experiments in the presence (Fig. 2, A and B) or absence (Fig. 2C) of 10% serum during the different treatments. Stable GFP-WIPI-1 U2OS cells were treated for 1, 2, or 3 h using five different concentrations for each drug. The concentrations for both TG and SP ranged between 0.02 and 0.5 $\mu$M, for SF, between 1 and 40 $\mu$M, and for EP, between 0.5 and 50 $\mu$M. As a positive control for the induction of autophagy, the cells were starved by using nutrient-free medium lacking amino acids and serum (NF); as a negative control for the inhibition of autophagy, wortmannin (233 nM) was used to inhibit PtdIns(3)P generation, which is a prerequisite for WIPI-1 to localize at autophagosomal membranes (Fig. 2). As expected, TG administration resulted in a significant increase in WIPI-1 puncta-positive cells after only 1 h using 0.02 $\mu$M TG in the presence of serum (Fig. 2B). Please note that short-term serum starvation already increases the number of WIPI-1 puncta-positive cells from ~10 to ~40% (Fig. 2, B and C, CM) and that under serum-free conditions, TG administration (0.02–0.5 $\mu$M) for 1 h did not lead to a significant increase of puncta-positive cells (Fig. 2C). However, 2- and 3-h TG administration also resulted in a significant increase of WIPI-1 puncta-positive cells in the absence of serum (Fig. 2C). This shows that the TG-promoted increase of WIPI-1 positive autophagosomal membranes over control conditions depends on the presence or absence of serum. This was also observed by using SP, SF, and ET (Fig. 2, B and C) and confirms previous data on the influence of serum during compound-mediated modulation of autophagy (Yang et al., 2010). SP treatments resulted in a significant increase of WIPI-1 puncta-positive cells, with a maximum increase of WIPI-1 puncta-positive cells when using 100 nM SP for 2 h in the presence (74%) or absence (84%) of serum (Fig. 2B). Cells treated with 0.25 and 0.5 $\mu$M staurosporine showed cell death-associated membrane blebbing (data not shown). SF administration also significantly increased the number of WIPI-1 puncta-positive cells, detectable using 5 $\mu$M for 2 h in the presence of serum (19%) and by using 10 to 40 $\mu$M for 1 to 3 h in both the presence and the absence of serum (Fig. 2, B and C). Treatment with 25 or 50 $\mu$M etoposide for 2 and/or 3 h resulted in a significant increase of WIPI-1 puncta-positive cells in the presence of serum (Fig. 2B); treatment with 1 to 50 $\mu$M etoposide for 2 and/or 3 h in serum-free medium resulted in a significant increase of puncta-positive cells (Fig. 2C).

Our results show that the effect on autophagy measured upon TG or SP application seems more prominent in the presence of serum; however, in the absence of serum, the overall basal level of autophagy is already increased, thereby diminishing the compound-mediated effect. In contrast, SF or EP treatments, especially those using lower concentra-

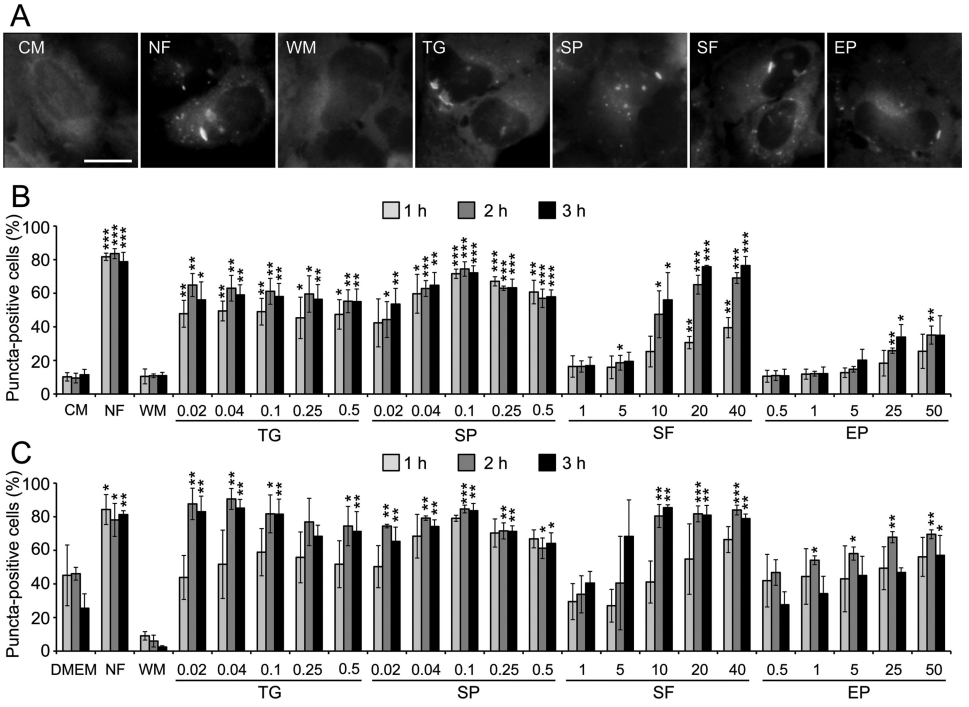


**Fig. 2.** Compound-mediated modulation of WIPI-1 puncta formation. The effect of thapsigargin, staurosporine, sorafenib, or etoposide treatment on WIPI-1 puncta formation was assessed in the presence (A and B) or absence of serum (C) over time. Stable GFP-WIPI-1 cells were treated with TG (0.02, 0.04, 0.1, 0.25, 0.5 $\mu$M), SP (0.02, 0.04, 0.1, 0.25, 0.5 $\mu$M), SF (1, 5, 10, 20, 40 $\mu$M), and EP (0.5, 1, 5, 25, 50 $\mu$M) for 1, 2, or 3 h. Nutrient starvation (NF) was used as positive control and WM treatment as negative control. Representative images from automated WIPI-1 puncta-formation analysis are shown. A, 40 nM TG, 100 nM SP, 40 $\mu$M SF, and 50 $\mu$M EP for 3 h. Up to 3000 individual cells were quantified for every single treatment; $n = 2$ to 3. B and C, $p$ Values: *, $p < 0.05$; **, $p < 0.01$; ***, $p < 0.001$. Scale bar, 20 $\mu$m.

tions, clearly resulted in a more prominent increase of WIPI-1 puncta-positive cells under serum-free conditions.

**$Ca^{2+}$ Chelation Inhibits Nutrient Starvation-Mediated Autophagy and the Effects of Pharmacological Compounds on WIPI-1 and LC3.** We reported previously that thapsigargin-mediated cytosolic $Ca^{2+}$ increase stimulated the localization of both WIPI-1 and LC3 at autophagosomal membranes (Grotemeier et al., 2010). Here, we sought to determine whether $Ca^{2+}$ availability is generally required for autophagosome formation. U2OS cells stably expressing GFP-WIPI-1 were incubated for 1 h with control medium (CM), NF, TG (40 nM), SP (100 nM), SF (40 $\mu$M) or wortmannin (WM; 233 nM) with or without 10 or 30 $\mu$M BAPTA-AM (Fig. 3, A–C). Automatically acquired fluorescence microscopy images are presented (Fig. 3A) as well as the heat map

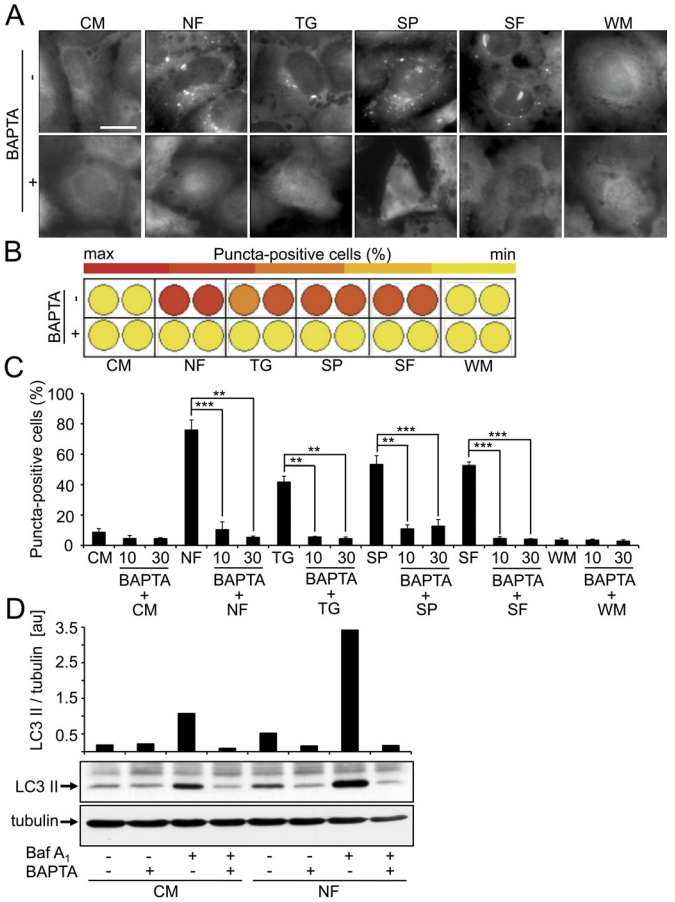


**Fig. 3.** $Ca^{2+}$ chelation prevents WIPI-1 and LC3 to localize at autophagosomal membranes. Stable U2OS GFP-WIPI-1 cells were pretreated with CM with or without BAPTA-AM (10 or 30 $\mu$M) for 30 min, followed by incubations for 1 h in control (CM) with or without TG (40 nM), SP (100 nM), SF (40 $\mu$M) or WM (233 nM) or in NF in the presence or absence of 10 and 30 $\mu$M BAPTA-AM. Cells were fixed and subjected to automated image acquisition (A). Images from treatments with 30 $\mu$M or without BAPTA-AM are presented along with automated WIPI-1 puncta-formation analysis (B and C). Dynamic heat map from automated WIPI-1 puncta-formation analysis (B). Up to 2600 individual cells were quantified for every single treatment; $n = 3$ (C). For LC3 lipidation analysis, U2OS osteosarcoma cells were pretreated with control medium with or without BAPTA-AM (30 $\mu$M), followed by treatments with Baf $A_1$ (200 nM) or Baf $A_1$ plus BAPTA-AM (30 $\mu$M) in CM or NF for 1 h. Cell lysates were subjected to Western blot analysis using anti-LC3 and anti-tubulin antibodies (D). Representative Western blot quantification from three independent experiments is shown (D), and supplemental information is available (Supplemental Fig. S1). $p$ Values: **, $p < 0.01$; ***, $p < 0.001$. Scale bar, 20 $\mu$m.

from automated WIPI-1 puncta-formation analyses (Fig. 3B) and the statistical analyses of up to 2600 individual cells per treatment (Fig. 3C). This quantification demonstrates that BAPTA-AM-mediated $Ca^{2+}$ chelation significantly prevents the increase of WIPI-1 puncta-positive cells upon NF, TG, SP, or SF treatments (Fig. 3C). In parallel, human U2OS osteosarcoma cells were treated with CM or NF for 1 h with or without BAPTA-AM; in addition, the autophagic flux was analyzed by introducing the lysosomal inhibitor Baf $A_1$ (Fig. 3D). We found that BAPTA-AM treatment drastically reduced LC3 lipidation under these conditions (Fig. 3D; Supplemental Fig. S1). These results imply that, in general, autophagy is prevented by $Ca^{2+}$ chelation, indicating that $Ca^{2+}$ availability is necessary for the induction of autophagy via WIPI-1 and LC3.

**Inhibition of CaMKI Signaling Reduces the Formation of WIPI-1 Positive Autophagosomal Membranes.** We found previously that the thapsigargin effect on WIPI-1 and LC3 is inhibited by using the selective CaMKK$\alpha/\beta$ inhibitor STO-609 (Grotemeier et al., 2010). Here, we used STO-609 during nutrient starvation of GFP-WIPI-1–expressing U2OS osteosarcoma cells (Fig. 4A). By automated analyses of up to 5100 individual cells, we found that STO-609 addition to NF, significantly reduced the number of GFP-WIPI-1 puncta-positive cells compared with NF alone (Fig. 4A, hatched symbols). However, even in the presence of STO-609 (10–30 $\mu$g/ml) nutrient starvation still significantly induced WIPI-1 puncta formation (Fig. 4A, star symbols).

This shows that CaMKK$\alpha/\beta$ inhibition partially reduces the nutrient-starvation-mediated formation of WIPI-1-positive autophagosomal membranes. Because CaMKK$\alpha/\beta$ acts upstream of AMPK, this result indicates that the $Ca^{2+}$/CaMKK$\alpha/\beta$/AMPK signaling cascade contributes to starvation-induced WIPI-1-positive autophagosomal membrane formation. Because the inhibition by STO-609 on WIPI-1 was partial, we investigated whether the AMPK-independent CaMK signaling route might also contribute to the regulation of WIPI-1. Administration of the selective CaMKI/II/IV inhibitor KN-93 (1, 5, or 10 $\mu$M) showed that 5 or 10 $\mu$M KN-93 significantly reduced the number of WIPI-1 puncta-positive cells induced by NF (Fig. 4B, hatched symbols). Again, this reduction was partial, as found using STO-609. However, because either selective inhibitor, STO-609 or KN-93, affected WIPI-1 puncta formation induced by nutrient starvation, our results indicate that CaMKI/IV (Means, 2008) also contributes to the regulation of WIPI-1. In support, STO-609 and KN-93 cotreatments (10, 20, or 30 $\mu$g/ml STO-609 in combination with 1, 5, or 10 $\mu$M KN-93) for 1 h in nutrient-free medium reduced WIPI-1 puncta-positive cells to basal control levels (Fig. 4B). Furthermore, autophagic flux assays on LC3 lipidation further confirmed this finding, in that LC3 lipidation decreased upon coadministration of STO-609 and KN-93 (Fig. 4C; Supplemental Fig. S2).

These results warranted address of the functional involvement of CaMKI and CaMKIV in regulating WIPI-1 by siRNA-mediated down-regulation. By introducing human siCaMKI or siCaMKIV in the GFP-WIPI-1 cell line, both proteins were prominently down-regulated; by combining siCaMKI and siCaMKIV, simultaneous down-regulation of CamKI/IV was achieved (Fig. 5A). Furthermore, upon 48 h of silencing, we treated the cells with CM or NF and coanalyzed the number of WIPI-1 puncta per puncta-positive cell (Fig.

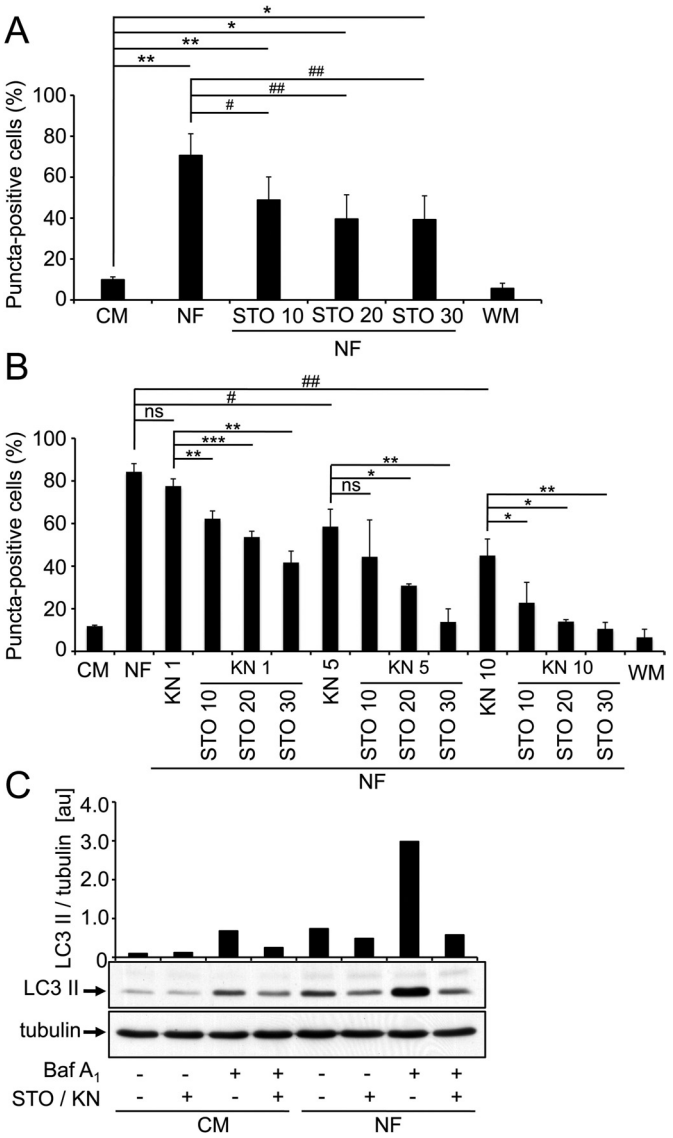


**Fig. 4.** Both STO-609, a selective inhibitor for CaMKK$\alpha/\beta$, and KN-93, a selective inhibitor for CaMKI/II/IV, reduced the localization of WIPI-1 and LC3 at autophagosomal membranes. Stable U2OS GFP-WIPI-1 cells were pretreated with CM with or without STO-609 (10, 20, or 30 $\mu$g/ml) for 30 min, followed by treatments using either CM or NF with or without STO-609 (10, 20, and 30 $\mu$g/ml) for 1 h. Automated WIPI-1 puncta-formation analysis of up to 5100 cells from every single treatment, $n = 4$ (A). $p$ Values: *, $p < 0.05$; **, $p < 0.01$ to CM; #, $p < 0.05$; ##, $p < 0.01$ to NF. Stable U2OS GFP-WIPI-1 cells were pretreated with CM with or without KN-93 (1, 5, and 10 $\mu$M), or combinations of STO-609 (10, 20, and 30 $\mu$g/ml) plus KN-93 (1, 5, and 10 $\mu$M) for 30 min. Subsequently, cells were treated with CM or NF with or without KN-93 (1, 5, and 10 $\mu$M), or combinations of STO-609 (10, 20, and 30 $\mu$g/ml) plus KN-93 (1, 5, and 10 $\mu$M) for 1 h. Automated WIPI-1 puncta-formation analysis of up to 2600 cells was quantified for every single treatment, $n = 3$ (B). $p$ Values: *, $p < 0.05$; **, $p < 0.01$; ***, $p < 0.001$; #, $p < 0.05$; ##, $p < 0.01$; $p \geq 0.05$ was not significant. In parallel, cotreatment of STO-609 and KN-93 was analyzed with regard to LC3 lipidation (B). U2OS cells were pretreated with CM with or without 30 $\mu$g/ml STO-609 plus 10 $\mu$M KN-93 for 30 min. Subsequently, cells were treated with Baf $A_1$ (200 nM), Baf $A_1$ (200 nM), and STO-609 (30 $\mu$g/ml) plus KN-93 (10 $\mu$M) in CM or NF for 1 h. Cell lysates were subjected to Western blot analysis using anti-LC3 and anti-tubulin antibodies. Representative Western blot quantification from three independent experiments is shown (C), and supplemental information is available (Supplemental Fig. S2).

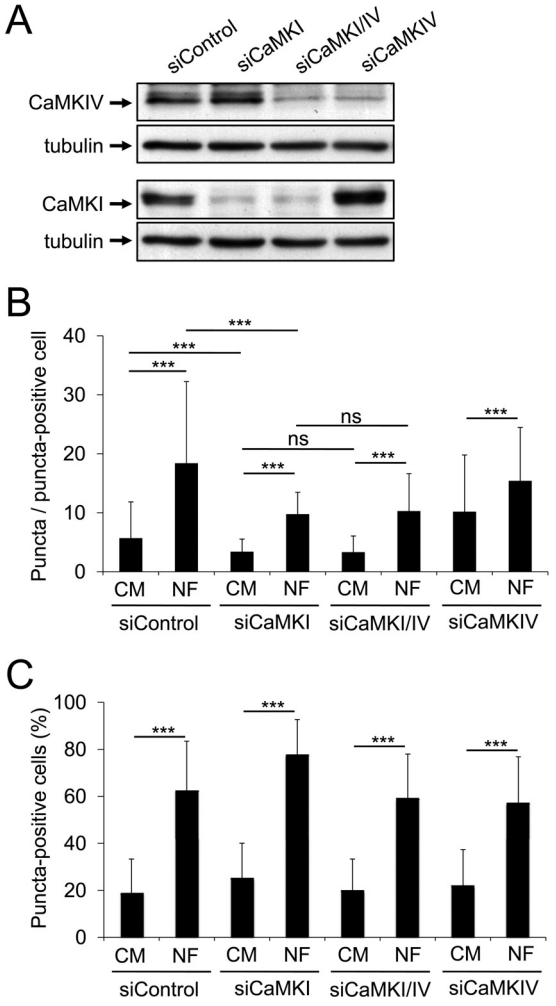


**Fig. 5.** Transient siRNA-mediated down-regulation of CaMKI reduces WIPI-1 puncta formation. Stable U2OS GFP-WIPI-1 cells were transiently transfected with 50 nM unique siRNAs (siControl, siCaMKI, siCaMKIV) or a combination of siCaMKI and siCaMKIV (each 25 nM) for 48 h. Protein extracts were subjected to Western blot analysis using anti-CaMKI, anti-CaMKIV, or anti-tubulin antibodies. Representative results are shown, $n = 2$ (A). Silenced cells were treated with CM and NF for 1 h followed by automated WIPI-1 puncta-formation analysis expressed as the number of GFP-WIPI-1 puncta per puncta-positive cell (B) or the number of GFP-WIPI-1 puncta-positive cells (C). Up to 3400 cells were analyzed for each treatment. Image fields from five to six independent experiments were used for both quantifications (B, C) and to calculate $p$ Values: ***, $p < 0.001$; $p \geq 0.05$ was not significant.

5B) or the number of WIPI-1 puncta-positive cells (Fig. 5C). Although imposed nutrient starvation resulted in a significant increase in the number of WIPI-1 puncta-positive cells (Fig. 5C), the number of WIPI-1 puncta per puncta-positive cell was significantly reduced in both nutrient-rich (CM) and NF conditions when CaMKI was down-regulated (Fig. 5B). Furthermore, although we observed a significant increase in WIPI-1 puncta per puncta-positive cell upon nutrient-starvation induced autophagy in siRNA-transfected cells targeting either CaMKI (siCaMKI), CaMKI/IV (siCaMKI/IV), or CaMKIV (siCaMKIV), this elevation was much less prominent compared with the siControl cells (Fig. 5B). This result, a partial inhibition of WIPI-1 puncta formation upon down-modulated CaMKI/IV protein levels, correlates with the partial inhibition of starvation-induced WIPI-1 puncta formation upon KN-93 treatment alone (Fig. 4B). The reduction of WIPI-1 puncta was not further lowered when CaMKIV was simultaneously down-regulated along with CaMKI (Fig. 5B), suggesting that the results achieved by using STO-609 and

KN-93 reflect the inhibition of CaMKI. However, down-regulation of CaMKIV alone also reduced the number of WIPI-1 puncta in nutrient-free medium (Fig. 5B), implying that in cells expressing CaMKIV in high abundance, such as neurons, CaMKIV might also contribute to the regulation of WIPI-1.

**Low AMPK$\alpha_1/\alpha_2$ Protein Levels Promote an Increase of Both WIPI-1 Puncta and LC3-II.** Next, we tested whether both LC3 lipidation and WIPI-1 puncta formation are dependent on AMPK. Therefore, we down-regulated human AMPK$\alpha_1/\alpha_2$ by siRNA-mediated transient transfection of GFP-WIPI-1 cells for 48 h and treated the cells with control or nutrient-free medium or with STO-609/KN-93 in nutrient-free medium (Fig. 6). We found that transiently reduced AMPK protein levels increase basal LC3 lipidation. Upon nutrient starvation, LC3 lipidation was further elevated, but this increase was sensitive to STO-609/KN-93 (Fig. 6A; Supplemental Fig. S3). By conducting autophagic flux assays, we confirmed that the increase of LC3-II upon siRNA-mediated transfection targeting AMPK (siAMPK) should not be due to the inhibition of autophagy, because bafilomycin $A_1$-mediated lysosomal inhibition promoted a further increase of both basal and nutrient starvation-induced LC3-II (data not shown). Using the same experimental setup, we simultaneously quantified the number of WIPI-1 puncta per puncta-positive cell (Fig. 6B) and the number of WIPI-1 puncta-positive cells (Fig. 6C). In line with increased LC3-II protein level upon transient down-regulation of AMPK, we found a significant increase of both WIPI-1 puncta per cell (Fig. 6B) and WIPI-1 puncta-positive cells (Fig. 6C). Again, nutrient-starvation induced WIPI-1 puncta formation was significantly reduced in the presence of STO-609/KN-93 (Fig. 6, B and C).

**AMPK$\alpha_1/\alpha_2$ Knockout Mouse Embryonic Fibroblasts Display Reduced WIPI-1 Puncta Formation under Basal Conditions.** AMPK$\alpha_1/\alpha_2$ wild-type (WT) and AMPK$\alpha_1/\alpha_2$-deficient MEFs (Laderoute et al., 2006) were transiently transfected with GFP-WIPI-1 for 24 h and treated with CM, NF, TG (100 nM), or WM (233 nM) for 3 h (Fig. 7, A and B). GFP-WIPI-1 puncta formation was assessed by confocal microscopy (Fig. 7B), showing that in the complete absence of AMPK$\alpha_1/\alpha_2$, WIPI-1 puncta formation was stimulated upon both nutrient starvation and cytosolic $Ca^{2+}$ increase by TG, and was inhibited by WM (Fig. 7B). However, the complexity of WIPI-1 puncta in WT and knockout MEFs differed (Fig. 7B). To quantify the formation of GFP-WIPI-1 puncta-positive cells, we transfected WT and AMPK$\alpha_1/\alpha_2$ knockout MEFs with GFP-WIPI-1 and cultured the cells for 24 h in control medium with high- or low-glucose concentrations as indicated in Fig. 7C (CM), followed by amino acid and serum starvation (NF) for 3 h and quantitative fluorescence microscopy (Fig. 7C). We found that the number of WIPI-1 puncta-positive cells was significantly reduced in AMPK$\alpha_1/\alpha_2$ knockout MEFs under nutrient-rich conditions, regardless of glucose concentrations (Fig. 7C). However, under nutrient-free conditions, autophagy was unaltered (Fig. 7C). This indicates that signaling cascades promoting the induction of autophagy by amino acid and serum starvation can bypass AMPK$\alpha_1/\alpha_2$, but that basal regulation of autophagy under nutrient-rich conditions involves AMPK$\alpha_1/\alpha_2$. This finding argues that the AMPK-TORC1 pathway also contributes to the regulation of WIPI-1. In support, by confocal microscopy studies on the colocalization of WIPI-1 and Atg1 (Ulk2), a target of both AMPK and TORC1, we found a partial colocalization of WIPI-1 and Ulk2 puncta (Fig. 8).

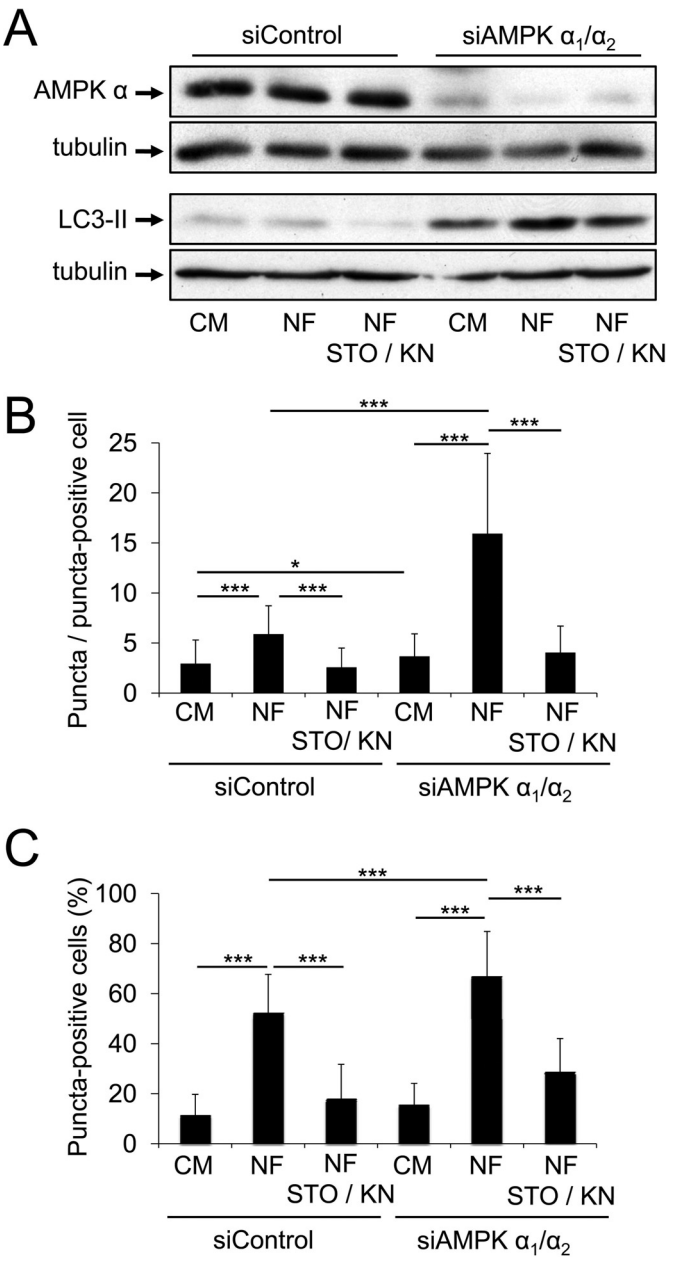


**Fig. 6.** Transient siRNA-mediated down-regulation of AMPK$\alpha_1/\alpha_2$ increased LC3 lipidation and WIPI-1 puncta formation. Stable U2OS GFP-WIPI-1 cells were transiently transfected with 50 nM unique siRNAs (siControl, AMPK$\alpha_1/\alpha_2$) for 48 h. Cells were pretreated with CM with or without 30 $\mu$g/ml STO-609 plus 10 $\mu$M KN-93 for 30 min. Subsequently, cells were treated with CM or NF with or without STO-609 (30 $\mu$g/ml) plus KN-93 (10 $\mu$M) for 1 h. Protein extracts were subjected to 8% (top) or 15% (bottom) SDS-polyacrylamide gel electrophoresis and Western blot analysis using anti-AMPK, anti-LC3, or anti-tubulin antibodies. Representative Western blot result ($n = 2$) is shown (A), and supplemental information is available (Supplemental Fig. S3). In parallel, automated WIPI-1 puncta-formation analysis was expressed as the number of GFP-WIPI-1 puncta per puncta-positive cell (B) or the number of GFP-WIPI-1 puncta-positive cells (C). Up to 2600 cells were analyzed for each treatment. Image fields from four independent experiments were used for both quantifications (B and C) and to calculate $p$ values: *, $p < 0.05$; ***, $p < 0.001$.

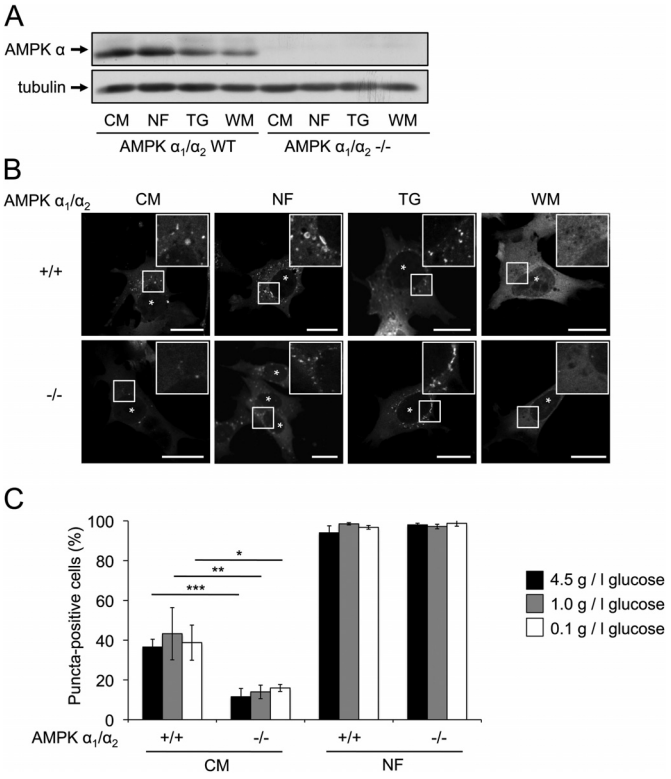


**Fig. 7.** AMPK$\alpha_1/\alpha_2$-deficient MEFs display reduced WIPI-1 puncta under nutrient-rich conditions. AMPK WT and AMPK$\alpha_1/\alpha_2$-deficient MEFs were subjected to anti-AMPK Western blotting confirming the absence of AMPK in knockout cells (A). AMPK WT and AMPK$\alpha_1/\alpha_2$-deficient MEFs were transiently transfected with GFP-WIPI-1 and treated with CM, NF, TG (100 nM), or WM. Representative images were acquired by confocal microscopy, $n = 3$ (B). Scale bars, 20 $\mu$m. Upon transient GFP-WIPI-1 transfection, AMPK WT and AMPK$\alpha_1/\alpha_2$-deficient MEFs were incubated for 24 h in CM with either 4.5, 1.0, or 0.1 g/l glucose medium and further treated with NF for 3 h or not. Quantitative fluorescence microscopy of 400 cells is presented, $n = 4$ (C). $p$ Values: *, $p < 0.05$; **, $p < 0.01$; ***, $p < 0.001$. Scale bars, 20 $\mu$m.

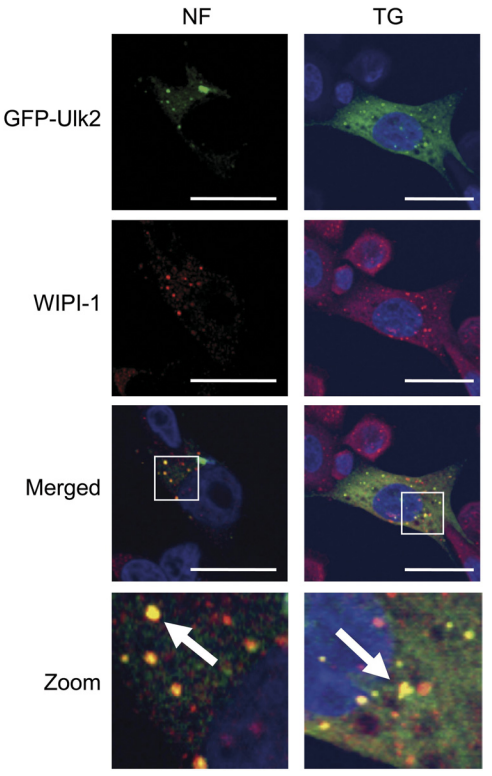


**Fig. 8.** Colocalization of endogenous WIPI-1/Alexa Fluor 546 (red) and overexpressed GFP-Ulk2 (green) upon nutrient starvation (NF) and TG treatment in human G361 cells. Nuclei were stained with TO-PRO-3 (blue). Arrows mark prominent colocalization of endogenous WIPI-1/Alexa Fluor 546 (red) and GFP-Ulk2 (green) (zoom). Scale bars, 20 $\mu$m.

## Discussion

Providing for macromolecules and energy, the process of cellular autophagy is constitutively active on a basal level. In response to a variety of imposed cellular stress, including nutrient and energy shortage, autophagic bulk degradation is induced above basal level to secure cellular survival. Alterations in the process of autophagy are associated with human diseases, such as cancer, neurodegeneration, and diseases of the heart, liver, and muscle (Mizushima et al., 2008). Alterations in autophagy genes have also been associated with human diseases, monoallelic deletions in *BECN1* with breast and ovarian cancer (Liang et al., 1999), and *ATG16L1* single-nucleotide polymorphism with Crohn's disease (Barrett et al., 2008; Cadwell et al., 2008). Although mutations in both genes contribute to different diseases, the encoded autophagosomal proteins Beclin 1 and Atg16L1 both function in the assembly of the autophagic machinery. The autophagosomal PtdIns(3)P-effector protein WIPI-1 is thought to function downstream of the Beclin 1/PtdIns3KC3 complex I and upstream of Atg16L (Nobukuni et al., 2007; Itakura and Mizushima, 2010) and might also be disease-associated because of its aberrant expression in analyzed matched normal/tumor patient tissues (Proikas-Cezanne et al., 2004). Activating the Beclin 1/PtdIns3KC3 complex I to generate PtdIns(3)P that is subsequently bound by PtdIns(3)P effectors, such as WIPI-1, is prerequisite for initiating canonical autophagosome formation (Proikas-Cezanne and Codogno, 2011). WIPI-1 is inhibited by counteracting PtdIns(3)P availability [wortmannin, 2-(4-morpholinyl)-8-phenyl-4*H*-1-benzopyran-4-one (LY294002)] or by mutating PtdIns(3)P-binding motifs in WIPI-1, and WIPI-1 is stimulated by rapamycin-mediated TORC1 inhibition (Proikas-Cezanne et al., 2007). TORC1 is the target of the energy sensor AMPK, both of which regulate autophagy via differential Atg1 (Ulk1) phosphorylation (Egan et al., 2011; Kim et al., 2011). This suggests that rapamycin-mediated stimulation of WIPI-1 should at least be partially guarded by this pathway, explaining that both amino acid and serum starvation lead to WIPI-1 stimulation (Fig. 2) and partial colocalization of WIPI-1 and Atg1 (Ulk2) (Fig. 8). Regarding autophagy regulation, the AMPK-TORC1 cascade was also shown to be triggered by $Ca^{2+}$/CaMKK$\alpha/\beta$ signaling (Høyer-Hansen et al., 2007). In line with this, we found that WIPI-1 is stimulated upon thapsigargin-mediated cytosolic $Ca^{2+}$ increase (Grotemeier et al., 2010). The different cellular stress situations we imposed by nutrient starvation (serum, amino acids) or pharmacological compound administration (sorafenib, staurosporine, thapsigargin) commonly depend on cytosolic $Ca^{2+}$ availability to increase the abundance of both WIPI-1 and LC3-positive autophagosomal membranes. Using nutrient starvation to trigger autophagy in the presence or absence of selective inhibitors (STO-609, KN-93), we found evidence for the involvement of the $Ca^{2+}$/calmodulin-CaMKI/IV cascade that is distinct from the $Ca^{2+}$/calmodulin-CaMKK$\alpha/\beta$-AMPK route. Both selective inhibitors applied alone significantly reduced the localization of WIPI-1 at autophagosomal

membranes upon nutrient starvation (Fig. 4). Although WIPI-1 puncta formation was not completely abolished upon either STO-609 or KN-93 alone, coapplication of STO-609 and KN-93 inhibited the induction of autophagy, measured by WIPI-1 puncta formation and LC3-II protein abundance (Fig. 4). It was suggested that an effect of KN-93 argues for an involvement of CaMKI/II/IV and rules out CaMKII if a similar effect is found with STO-609 (Means, 2008). However, CaMKII has long been suggested to be involved in autophagy (Holen et al., 1992). By using siRNA-mediated down-regulation of CaMKI and CaMKIV, we found that the function of CaMKI indeed contributes to the formation of WIPI-1 positive autophagosomal membranes (Fig. 5). It is noteworthy that although the number of WIPI-1 puncta per cell significantly increased upon nutrient starvation in siRNA-transfected cells targeting CaMKI, this elevation was prominently reduced compared with the siControl setting. In support, KN-93 treatment also resulted in a partial inhibition of WIPI-1 puncta-formation. This shows that CaMKI signaling is involved in the regulation of WIPI-1 mediated autophagy, but complete inhibition is not achieved by siRNA-mediated CaMKI down-regulation or by the use of selective inhibitors alone. Full inhibition is achieved only upon BAPTA-AM-mediated chelation of intracellular $Ca^{2+}$ or upon PtdIns(3)P depletion (Fig. 3).

However, our results demonstrate that CaMKs contribute in part to the regulation of WIPI-1-mediated autophagy. In line with $Ca^{2+}$ signaling opportunities via CaMKs in the absence of AMPK, we found that nutrient starvation-mediated autophagy can take place in AMPK$\alpha_1/\alpha_2$ mouse embryonic fibroblasts from knockout mice compared with the wild-type control (Fig. 7). However, basal autophagy was significantly reduced in the AMPK$\alpha_1/\alpha_2$-deficient background (Fig. 7). This result indicates that starvation-induced autophagy can bypass AMPK$\alpha_1/\alpha_2$, either because catalytic subunits of AMPK-related protein kinase family members (Dale et al., 1995) substitute for AMPK$\alpha_1/\alpha_2$ function or because AMPK$\alpha_1/\alpha_2$ deficiency reflects an AMPK-null background as suggested (Laderoute et al., 2006). However, because the localization of WIPI-1 at autophagosomal membranes under nutrient-rich conditions is significantly reduced without AMPK$\alpha_1/\alpha_2$, AMPK should be a crucial regulatory factor for basal autophagy. Furthermore, by siRNA-mediated transient down-regulation of AMPK$\alpha_1/\alpha_2$, we found an increase of both autophagosomal markers LC3-II protein and WIPI-1 positive membranes, arguing that low AMPK$\alpha_1/\alpha_2$ protein levels might induce autophagy, prominently under nutrient-free conditions (Fig. 6). It is tempting to speculate that evolutionary highly conserved pathways, such as generation of PtdIns(3)P and AMPK-mediated mTOR inhibition, regulate basal autophagy and consequently promote adaptation to nutrition/energy supply; additional and distinct signal cascades such as $Ca^{2+}$ mobilization via CaMKI/IV that we found here to contribute to the regulation of WIPI-1 and LC3, independent of AMPK, might present further signaling opportunities to modulate autophagy. In fact, noncanonical pathways that modulate autophagy but bypass canonical Atg proteins have been identified (e.g., Nishida et al., 2009). It is noteworthy that the study (Nishida et al., 2009) that provides evidence for an Atg5/Atg7-independent entry into autophagic sequestration upon etoposide treatment depends on the activity of PtdIns3KC3 to generate PtdIns(3)P. In line with this, we found in the current study that etoposide treatment increases the number of cells in which WIPI-1 localizes at autophagosomal membranes, suggesting that WIPI-1 marks also noncanonical autophagy pathways as long as PtdIns(3)P is generated. Forced cellular stress by further compounds (etoposide, sorafenib, staurosporine, thapsigargin) or nutrient starvation (amino acids, serum) always increased the number of WIPI-1 puncta-positive cells, and $Ca^{2+}$ chelation nullified the localization of WIPI-1 at autophagosomal membranes; in line with this, LC3-II protein abundance was also decreased upon $Ca^{2+}$ chelation (current study). The most compelling interpretation from this might be that all of the treatments employed promote $Ca^{2+}$ mobilization from intracellular stores and modulate autophagy. Work from Park et al. (2008) regarding the molecular characterization of sorafenib-treated tumor cells demonstrated that sorafenib promotes both autophagy and cell death by acting synergistically with vorinostat. Staurosporine treatment has long been correlated with both autophagy and cell death, reporting the appearance of autophagosomes upon staurosporine treatment (30 nM) for 22 to 28 h in *Tetrahymena thermophila* and apoptotic cell blebbing between 12 and 44 h (Christensen et al., 1998). Our current study demonstrates that both starvation-induced and pharmacological compound-modulated autophagy depends on the availability of cytosolic $Ca^{2+}$ to permit the localization of WIPI-1 (Proikas-Cezanne and Robenek, 2011) and LC3 at autophagosomal membranes. WIPI-1 should be regulated by 1) PtdIns(3)P generation, 2) $Ca^{2+}$ mobilization, and 3) mTOR inhibition, indicating that WIPI-1 functions as a PtdIns(3)P effector that receives additional required signals during regulated autophagosome formation (see our proposed model in Supplemental Fig. S4). The current study provides evidence for this hypothesis and for an involvement of CaMKI independent of AMPK. In light of future putative employment of therapeutical compounds to modulate autophagy, stimulating $Ca^{2+}$ signaling might represent a further opportunity to influence this cellular process.

**Acknowledgments**

We are grateful to Benoit Viollet (Université Paris Descartes, Paris, France) for providing the AMPK-deficient and wild-type mouse embryonic fibroblasts and for helpful comments on the manuscript. We thank Katharina Hentschel for technical assistance.

**Authorship Contributions**

*Participated in research design*: Codogno and Proikas-Cezanne.
*Conducted experiments*: Pfisterer and Mauthe.
*Performed data analysis*: Pfisterer, Mauthe, and Proikas-Cezanne.
*Wrote or contributed to the writing of the manuscript*: Pfisterer and Proikas-Cezanne.

**References**

Barrett JC, Hansoul S, Nicolae DL, Cho JH, Duerr RH, Rioux JD, Brant SR, Silverberg MS, Taylor KD, Barmada MM, et al. (2008) Genome-wide association defines more than 30 distinct susceptibility loci for Crohn's disease. *Nat Genet* **40:**955–962.
Blommaart EF, Krause U, Schellens JP, Vreeling-Sindelárová H, and Meijer AJ (1997) The phosphatidylinositol 3-kinase inhibitors wortmannin and LY294002 inhibit autophagy in isolated rat hepatocytes. *Eur J Biochem* **243:**240–246.
Blommaart EF, Luiken JJ, Blommaart PJ, van Woerkom GM, and Meijer AJ (1995) Phosphorylation of ribosomal protein S6 is inhibitory for autophagy in isolated rat hepatocytes. *J Biol Chem* **270:**2320–2326.
Brady NR, Hamacher-Brady A, Yuan H, and Gottlieb RA (2007) The autophagic response to nutrient deprivation in the hl-1 cardiac myocyte is modulated by Bcl-2 and sarco/endoplasmic reticulum calcium stores. *FEBS J* **274:**3184–3197.
Cadwell K, Liu JY, Brown SL, Miyoshi H, Loh J, Lennerz JK, Kishi C, Kc W, Carrero JA, Hunt S, et al. (2008) A key role for autophagy and the autophagy gene Atg16l1 in mouse and human intestinal Paneth cells. *Nature* **456:**259–263.
Chen Y and Klionsky DJ (2011) The regulation of autophagy - unanswered questions. *J Cell Sci* **124:**161–170.

Christensen ST, Chemnitz J, Straarup EM, Kristiansen K, Wheatley DN, and Rasmussen L (1998) Staurosporine-induced cell death in Tetrahymena thermophila has mixed characteristics of both apoptotic and autophagic degeneration. *Cell Biol Int* **22:**591–598.
Codogno P, Ogier-Denis E, and Houri JJ (1997) Signal transduction pathways in macroautophagy. *Cell Signal* **9:**125–130.
Dale S, Wilson WA, Edelman AM, and Hardie DG (1995) Similar substrate recognition motifs for mammalian AMP-activated protein kinase, higher plant HMG-CoA reductase kinase-A, yeast SNF1, and mammalian calmodulin-dependent protein kinase I. *FEBS Lett* **361:**191–195.
Demarchi F, Bertoli C, Copetti T, Tanida I, Brancolini C, Eskelinen EL, and Schneider C (2006) Calpain is required for macroautophagy in mammalian cells. *J Cell Biol* **175:**595–605.
Egan DF, Shackelford DB, Mihaylova MM, Gelino S, Kohnz RA, Mair W, Vasquez DS, Joshi A, Gwinn DM, Taylor R, et al. (2011) Phosphorylation of ULK1 (hATG1) by AMP-activated protein kinase connects energy sensing to mitophagy. *Science* **331:**456–461.
Fleming A, Noda T, Yoshimori T, and Rubinsztein DC (2011) Chemical modulators of autophagy as biological probes and potential therapeutics. *Nat Chem Biol* **7:**9–17.
Grotemeier A, Alers S, Pfisterer SG, Paasch F, Daubrawa M, Dieterle A, Viollet B, Wesselborg S, Proikas-Cezanne T, and Stork B (2010) AMPK-independent induction of autophagy by cytosolic $Ca^{2+}$ increase. *Cell Signal* **22:**914–925.
Hardie DG (2008) Role of AMP-activated protein kinase in the metabolic syndrome and in heart disease. *FEBS Lett* **582:**81–89.
Holen I, Gordon PB, and Seglen PO (1992) Protein kinase-dependent effects of okadaic acid on hepatocytic autophagy and cytoskeletal integrity. *Biochem J* **284:**633–636.
Høyer-Hansen M, Bastholm L, Szyniarowski P, Campanella M, Szabadkai G, Farkas T, Bianchi K, Fehrenbacher N, Elling F, Rizzuto R, et al. (2007) Control of macroautophagy by calcium, calmodulin-dependent kinase kinase-beta, and Bcl-2. *Mol Cell* **25:**193–205.
Itakura E and Mizushima N (2010) Characterization of autophagosome formation site by a hierarchical analysis of mammalian Atg proteins. *Autophagy* **6:**764–776.
Khan MT and Joseph SK (2010) Role of inositol trisphosphate receptors in autophagy in DT40 cells. *J Biol Chem* **285:**16912–16920.
Kim J, Kundu M, Viollet B, and Guan KL (2011) AMPK and mTOR regulate autophagy through direct phosphorylation of Ulk1. *Nat Cell Biol* **13:**132–141.
Klionsky DJ, Cuervo AM, Dunn WA Jr, Levine B, van der Klei I, and Seglen PO (2007) How shall I eat thee? *Autophagy* **3:**413–416.
Klionsky DJ and Emr SD (2000) Autophagy as a regulated pathway of cellular degradation. *Science* **290:**1717–1721.
Kondo Y, Kanzawa T, Sawaya R, and Kondo S (2005) The role of autophagy in cancer development and response to therapy. *Nat Rev Cancer* **5:**726–734.
Laderoute KR, Amin K, Calaoagan JM, Knapp M, Le T, Orduna J, Foretz M, and Viollet B (2006) 5′-AMP-activated protein kinase (AMPK) is induced by low-oxygen and glucose deprivation conditions found in solid-tumor microenvironments. *Mol Cell Biol* **26:**5336–5347.
Liang XH, Jackson S, Seaman M, Brown K, Kempkes B, Hibshoosh H, and Levine B (1999) Induction of autophagy and inhibition of tumorigenesis by beclin 1. *Nature* **402:**672–676.
Matsunaga K, Saitoh T, Tabata K, Omori H, Satoh T, Kurotori N, Maejima I, Shirahama-Noda K, Ichimura T, Isobe T, et al. (2009) Two Beclin 1-binding proteins, Atg14L and Rubicon, reciprocally regulate autophagy at different stages. *Nat Cell Biol* **11:**385–396.
Means AR (2008) The Year in Basic Science: calmodulin kinase cascades. *Mol Endocrinol* **22:**2759–2765.
Mizushima N, Levine B, Cuervo AM, and Klionsky DJ (2008) Autophagy fights disease through cellular self-digestion. *Nature* **451:**1069–1075.
Nakatogawa H, Ichimura Y, and Ohsumi Y (2007) Atg8, a ubiquitin-like protein required for autophagosome formation, mediates membrane tethering and hemifusion. *Cell* **130:**165–178.
Nishida Y, Arakawa S, Fujitani K, Yamaguchi H, Mizuta T, Kanaseki T, Komatsu M, Otsu K, Tsujimoto Y, and Shimizu S (2009) Discovery of Atg5/Atg7-independent alternative macroautophagy. *Nature* **461:**654–658.
Nobukuni T, Kozma SC, and Thomas G (2007) hvps34, an ancient player, enters a growing game: mTOR Complex1/S6K1 signaling. *Curr Opin Cell Biol* **19:**135–141.
Noda T, Matsunaga K, Taguchi-Atarashi N, and Yoshimori T (2010) Regulation of membrane biogenesis in autophagy via PI3P dynamics. *Semin Cell Dev Biol* **21:**671–676.
Ohsumi Y (2001) Molecular dissection of autophagy: two ubiquitin-like systems. *Nat Rev Mol Cell Biol* **2:**211–216.
Park MA, Zhang G, Martin AP, Hamed H, Mitchell C, Hylemon PB, Graf M, Rahmani M, Ryan K, Liu X, et al. (2008) Vorinostat and sorafenib increase ER stress, autophagy and apoptosis via ceramide-dependent CD95 and PERK activation. *Cancer Biol Ther* **7:**1648–1662.
Petiot A, Ogier-Denis E, Blommaart EF, Meijer AJ, and Codogno P (2000) Distinct classes of phosphatidylinositol 3′-kinases are involved in signaling pathways that control macroautophagy in HT-29 cells. *J Biol Chem* **275:**992–998.
Proikas-Cezanne T and Codogno P (2011) Beclin 1 or not Beclin 1… *Autophagy* **7:**671–672.
Proikas-Cezanne T and Robenek H (2011) Freeze-fracture replica immunolabelling reveals human WIPI-1 and WIPI-2 as membrane proteins of autophagosomes. *J Cell Mol Med* doi:10.1111/j.1582-4934.2011.01339.x.
Proikas-Cezanne T, Ruckerbauer S, Stierhof YD, Berg C, and Nordheim A (2007) Human WIPI-1 puncta-formation: a novel assay to assess mammalian autophagy. *FEBS Lett* **581:**3396–3404.
Proikas-Cezanne T, Waddell S, Gaugel A, Frickey T, Lupas A, and Nordheim A (2004) WIPI-1alpha (WIPI49), a member of the novel 7-bladed WIPI protein family, is aberrantly expressed in human cancer and is linked to starvation-induced autophagy. *Oncogene* **23:**9314–9325.
Rubinsztein DC, Cuervo AM, Ravikumar B, Sarkar S, Korolchuk V, Kaushik S, and Klionsky DJ (2009) In search of an "autophagomometer". *Autophagy* **5:**585–589.
Williams A, Sarkar S, Cuddon P, Ttofi EK, Saiki S, Siddiqi FH, Jahreiss L, Fleming A, Pask D, Goldsmith P, et al. (2008) Novel targets for Huntington's disease in an mTOR-independent autophagy pathway. *Nat Chem Biol* **4:**295–305.
Yang J, Takahashi Y, Cheng E, Liu J, Terranova PF, Zhao B, Thrasher JB, Wang HG, and Li B (2010) GSK-3beta promotes cell survival by modulating Bif-1-dependent autophagy and cell death. *J Cell Sci* **123:**861–870.

**Address correspondence to:** Tassula Proikas-Cezanne, Autophagy Laboratory, Interfaculty Institute for Cell Biology, Eberhard Karls University Tuebingen, Auf der Morgenstelle 15, 72076 Tuebingen, Germany. E-mail: tassula.proikas-cezanne@uni-tuebingen.de